Horizontal Curvature Impacts on Steel Plate Girder Shear Buckling

Bernard A. Frankl[1], Daniel G. Linzell[2]

Abstract
Current provisions for shear design of slender, steel, plate girders do not account for effects from horizontal curvature, sometimes resulting in overly conservative designs. Excess transverse stiffeners are often specified and, since they are welded to the girder web, an increased risk of fatigue could exist. This manuscript summarizes a study that investigated horizontal curvature effects on shear behavior of steel plate girders having slender webs. Two shear buckling coefficients that include these effects are presented and compared against curved girder finite element models. Results show horizontal curvature increases shear buckling capacity and ultimate shear strength over a range of girder horizontal curvatures, web slenderness ratios and panel aspect ratios. These enhanced capacities could be utilized to reduce the number of transverse stiffeners needed to resist construction and service load demands.

1. Introduction

Due to increased fabrication and erection costs, steel bridges have had to become more structurally efficient over time to remain competitive. This is even true for specialized segments of the industry where steel had traditionally offered an advantage, such as for horizontally curved, plate girder bridges. In the United States, effects of horizontal curvature on plate girder behavior were extensively studied by the Consortium of University Research Teams (CURT) in the 1960's (Culver, 1972) and by the Curved Steel Bridge Research Project (CSBRP) in the late 1990's and early 2000's (Hall & Yoo, 1998). Both of these projects naturally focused on how horizontal curvature affected flexural behavior. Horizontal curvature effects on shear behavior were largely ignored. Some studies outside of these efforts have examined horizontal curvature influence on shear behavior, including studies by Legget and Batdorf et.al. (Batdorf, Stein, & Schildcrout, 1947; Leggett, 1937), however, larger, parameterized examinations have not been identified in the literature.

Classical formulations predicting the shear capacity of flexural members subject to small displacements were first developed by Barre de Saint-Venant in 1843 (de Saint-Venant, 1843; Hibbeler, 2005). In 1916, Rode developed a Pratt Truss formulation modeling post-buckling behavior of slender steel webs, termed Tension Field Action (TFA) (Rode, 1916). TFA was applied to steel girder design via Basler's Pratt Truss Analogy in 1961. This version of Basler's work

---

[1] HDR, Bridge Engineer, <bernard.frankl@hdrinc.com>
[2] Volte-Keegan Professor and Chair, Department of Civil Engineering, The University of Nebraska-Lincoln, <dlinzell@unl.edu>

incorporated Vincent's simplification of Bleich's shear buckling coefficient (Basler, 1961; Bleich, 1952; Vincent, 1969). Vincent's work simplified Bleich's piecewise solution to a single equation for design implementation.

While multiple studies have focused on predicting pre- and post-buckling shear capacity of steel plate girders having slender, straight, webs, limited research has focused on curved webs in shear. One of the more prominent studies was a series of tests completed by Jung and White (Jung & White, 2006). They examined four horizontally curved girders having a 36 ft (11.52 m) span length and web radii of 120.00 ft (36.57 m) and 208.75 ft (63.63 m). The girders were tested as propped, simply-supported sections with simply supported spans of 24 ft (73.16 m) with 12 ft (36.58 m) cantilevered sections as shown in Figure 1. Cross sections consisted of 0.34 in (8.53 mm) by 47.91 in (1217.00 mm) webs and 21.52 in (546.60 mm) by 0.91 in (22.99 mm) flanges, resulting in a web slenderness ratio of 150. Lateral bracing was provided at 12 ft (3.66 m) intervals with transverse stiffeners and connection plates placed to produce panel aspect ratios of 1.5 and 3.0 as shown in Table 1. To generate larger shears over the interior support, loads were applied at the center of the simply supported span and the end of the cantilever, with the mid-span load being 3-times the cantilever load.

Table 1: Girder Parameters (Jung & White, 2006)

Specimen	Radius, ft (m)	D/t_w	d_o/D	d_o/R
S1	208.75 (63.63)	142.59	3.0	0.0575
S1-S	208.75 (63.63)	143.99	1.5	0.0300
S2	120.00 (36.57)	146.51	3.0	0.1000
S2-S	120.00 (36.57)	147.87	1.5	0.0500
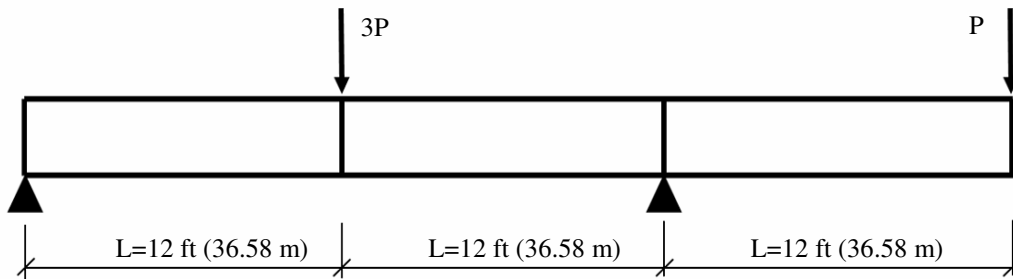
Figure 1: Test Setup (Jung & White, 2006)

Jung and White reported linearly elastic behavior until the onset of web buckling in the high shear region. Shear strength continued to increase in a nonlinear fashion until ultimate strength was reached, followed by specimen softening. Jung and White established the critical shear buckling load using calibrated FEM eigenvalue buckling analyses. Their findings showed horizontal curvature had minor effects on shear capacity for the girders that were tested.

More extensive, computational studies of the effects of horizontal curvature on shear resistance of very slender webs (slenderness ratios above 300) occurred for the aircraft industry. Specifically, Batdorf et al. (Batdorf et al., 1947) developed a shear buckling coefficient for slender, steel panels utilizing energy principles that incorporated a trigonometric shape function and the Galerkin

method. However, as stated earlier, effects of horizontal curvature on slender, curved, webs have not been extensively examined parametrically.

This paper provides an overview of a study that investigated effects of horizontal curvature on web shear behavior and corresponding shear capacity of steel plate girders. Summarized herein is research that developed simplified and a detailed equations for the shear buckling coefficient. The coefficients were developed in a form compatible with the current shear buckling coefficient equation used in the American Association of State Highway and Transportation Officials (AASHTO) *LRFD Bridge Design Specifications* (AASHTO, 2014). Developed coefficients were used to calculate capacities that were compared against results from a series of FEM models of plate girders having varying horizontal curvatures, web slenderness ratios and panel aspect ratios, showing favorable results.

2. Simplified Shear Buckling Coefficient
As stated earlier, computational studies have examined horizontal curvature effects on shear in slender, steel webs but not in the context of steel, plate girder webs. This study considered the behavior of panels with slenderness ratios up to the AASHTO limiting value of 300 and initially developed a simplified approximation of Batdorf's shear buckling coefficient, which was subsequently reformulated to match current AASHTO specifications.

As mentioned earlier, Batdorf (Batdorf et al., 1947) utilized energy principles to develop a curved web shear buckling coefficient. In doing so, he formulated the horizontal curvature parameter (Z) shown in (Eq. 1). This parameter combined important variables, including web slenderness, D/t_w, girder radius, R, and Poisson's ratio, ν, to quantify the extent of horizontal curvature coupled with the girder's shear sensitivity to that curvature.

$$Z = \frac{D^2}{Rt_w}\sqrt{1-\nu^2}. \tag{1}$$

Sinusoidal shape functions were developed to represent buckling modes and the Galerkin method was employed to approximate energy based solutions to resulting differential equations. A series of homogeneous, linear, algebraic equations were produced for an infinite number of buckled shapes. Minimization of these equations produced the critical shear buckling coefficient for each panel aspect ratio, d_o/D, where d_o is the panel length between stiffeners, and horizontal curvature parameter pair. Batdorf simplified the rigorous computational process by developing shear buckling coefficient curves as a function of Z and d_o/D. The curves are reproduced for panel aspect ratios greater than or equal to 1 as the dashed lines in Figure 2.
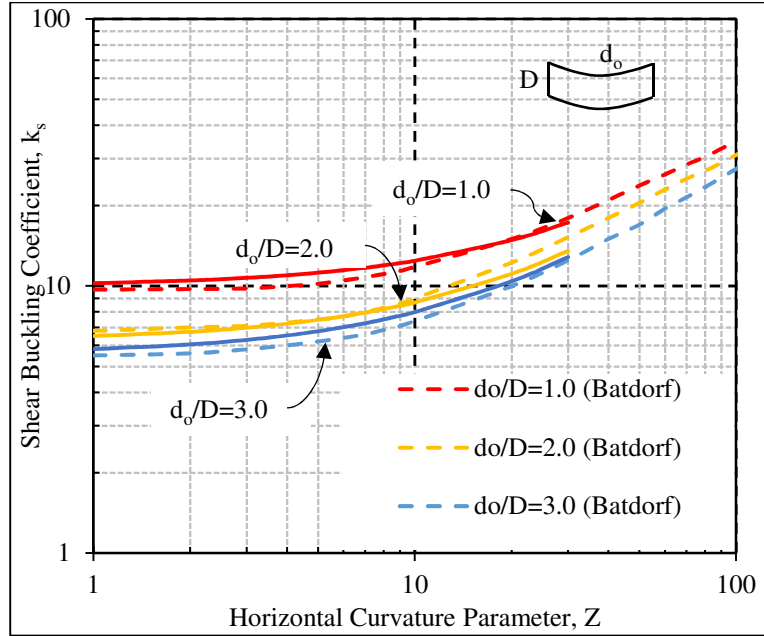
Figure 2: Comparison between Batdorf and Proposed Shear Buckling Coefficient Curves

The current study initially reproduced Batdorf's curves for horizontal curvature parameters between 1 and 1000. AASHTO (AASHTO, 2014) imposes geometric limits on girder horizontal curvature, web slenderness and panel aspect ratio. Consideration of these limits narrowed the range of applicable horizontal curvature parameters as summarized in Table 2, which shows a maximum Z of 30 when plate girder depths ranged between the common values of 48 in. (1219 mm) and 180 in. (4572 mm). Consequently, Figure 2 only shows Batdorf's curves through a Z of 100.

Table 2: Horizontal Curvature Parameter (Z) for FEM Girders

D, in (mm)	t_w, in (mm)		D/t_w	R, in (mm)		Z
48	0.32	(8)	150	1800	(45720)	3.82
(1219)	0.16	(4)	300	1800	(45720)	7.63
84	0.56	(14)	150	1800	(45720)	6.68
(2134)	0.28	(7)	300	1800	(45720)	13.36
120	0.8	(20)	150	1800	(45720)	9.54
(3048)	0.4	(10)	300	1800	(45720)	19.08
156	1.04	(26)	150	1800	(45720)	12.40
(3962)	0.52	(13)	300	1800	(45720)	24.80
180	1.2	(30)	150	1800	(45720)	14.31
(4572)	0.6	(15)	300	1800	(45720)	28.62

The current study initially regressed Batdorf's curves into an equation compatible with AASHTO shear design equations for Z between 1 and 30. Y-intercepts in Figure 2 represented the buckling coefficient for Z equal to 1, a "straight" girder. A polynomial regression function was used to approximate each curve with a resulting, generalized shear buckling coefficient equation formulated so it reduced to AASHTO's coefficient equation for straight girders. Based on the

regression, an additional term was derived and added to the current AASHTO equation as shown in Eq. (2). When compared against Batdorf's curves as shown in Figure 2, this equation showed good agreement.

$$k_s = 5 + \frac{5}{\left(\frac{d_o}{D}\right)^2} + 0.24 \frac{D^2}{Rt_w} \quad \text{where } Z \leq 30. \tag{2}$$

An in-depth discussion regarding development of this shear buckling coefficient is provided in Frankl (Frankl, 2017).

3. Detailed Shear Buckling Coefficient

The second approach used to obtain the shear buckling coefficient initiated with Timoshenko's energy-based derivation in the 1930's. This approach was selected because Timoshenko's derivation is the basis for shear buckling coefficients currently used in multiple bridge design standards and specifications, including AASHTO.

The current, detailed formulation directly accounted for horizontal curvature in the web (shear) panel displacement function that was used to derive the shear strain energy and external work equations shown in Eq. (3) and Eq. (4). Directly accounting for horizontal curvature was accomplished by superimposing initial displacement functions onto Timoshenko's functions as shown in Figure 3.
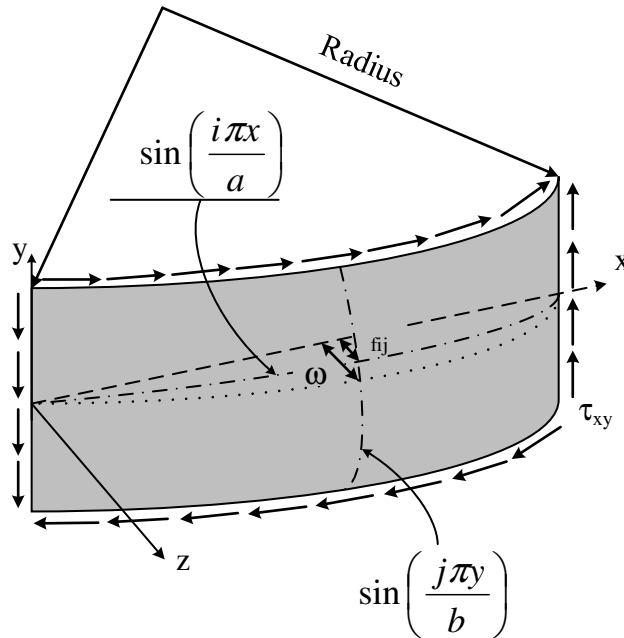
Figure 3: Shear panel displacement functions

The resulting displacement function is comprised of two terms as shown in Eq. (3). The first term represents web displacement through its depth. The second term represents an initial out-of-plane displacement along the length, indicative of horizontal curvature.

5

$$w = \sum\nolimits_{i=1}^{n} \sum\nolimits_{j=1}^{n} f_{ij}\sin\frac{i\pi x}{a}\sin\frac{j\pi y}{b} + \sum\nolimits_{i=1}^{n} \sum\nolimits_{j=1}^{n} f_{ij}\omega\sin\frac{i\pi x}{a}, \qquad (3)$$

where i and j represent an even and odd mode shape order respectively, x and y represent horizontal and vertical coordinates within a web panel, f_{ij} is a mode shape scaling factor, and ω represents the magnitude of horizontal curvature across the panel length, $\omega = R - R\cos\left(\frac{a}{2R}\right)$. Work and strain energy equations appear as:

$$U_w = -\tau_{xy}t\int_0^a\int_0^b \frac{\partial w}{\partial x}\frac{\partial w}{\partial y}dxdy, \qquad (4)$$

$$V = \frac{D_t}{2}\int_0^a\int_0^b\left\{\left(\frac{\partial^2 w}{\partial x^2} + \frac{\partial^2 w}{\partial y^2}\right)^2\right\}dxdy, \qquad (5)$$

where U_w is strain energy potential, V is work performed by the panel deformations under applied shear loads, τ_{xy} is the shear stress, D_t is the plate's flexural rigidity ($D_t = \frac{Et_w}{12(1-v^2)}$) and E is the modulus of elasticity. Equating the two and applying energy minimization principles produces a plate buckling equation that can be reformulated to solve for the shear buckling coefficient. This is accomplished via application of simply-supported edge conditions and by grouping terms so the first term reproduces Timoshenko's classical formulation for the buckling stress of an infinitely long plate. Additional, higher order, terms that result include horizontal curvature effects. When reformulated to determine k_s, the equation appears as shown in Eq. (6).

$$k_s = \frac{9\pi^2 Dt_w}{288d_o^2}\left(4(1+\alpha^2)^2 + \frac{\sqrt{128}\omega}{\pi}\sqrt{1+\alpha^2}\sqrt{4+4\alpha^2} + 8\omega^2\right). \qquad (6)$$

Timoshenko found that his infinite plate shear buckling solution overestimated experimental shear buckling capacities by approximately 15% and, as a result, reduced k_s accordingly. A similar reduction was adopted for the first term in Eq. (6). Additional terms in the equation were calibrated via comparisons against a series of FEM analyses of girders having varying values for Z and web slenderness and panel aspect ratios, with variable ranges falling within AASHTO (AASHTO, 2014) limits. Calibration steps are summarized in the paragraphs that follow.

A total of 10 girders, shown in Table 3, were analyzed. Z fell between 2.6 to 28.6 for these girders, with web slenderness ratios between 143 to 300 and panel aspect ratios either 1.5 or 3.0. Corresponding web depths were between 47.9 in (1217 mm) and 180 in (4572 mm). The girders were modelled in ABAQUS CAE (*ABAQUS/CAE*, 2013) using 4-noded shell elements with reduced integration (S4R elements). The models included initial imperfections adopted from the American Welding Society (AWS) *D1.1:200: Structural Welding Code – Steel* (*American Welding Society*, 2015) and residual stresses taken from the European Convention for Construction

Steelwork (ECCS) (Issa-El-Khoury, 2010; Jung & White, 2006). The FEM model was calibrated against results from Jung & White's tests and details are found in Frankl (Frankl, 2017).

Table 3: Girder Parameters

Girder	D,in (mm)	t_w, in (mm)	d_o, in (mm)	R, ft (m)	D/t_w	d_o/D	Z	k_s
S1	47.91 (1217)	0.336 (9)	144 (3658)	208.75 (63.62)	143	3.0	2.6	6.2
S1-S	47.95 (1218)	0.333 (8)	72 (1829)	208.75 (63.63)	144	1.5	2.6	7.9
UNL1	75 (1905)	0.25 (6)	225 (5715)	400 (121.92)	300	3.0	4.5	6.7
UNL2	75 (1905)	0.25 (6)	112.5 (2858)	400 (121.92)	300	1.5	4.5	8.4
UNL3	75 (1905)	0.25 (6)	225 (5715)	150 (45.72)	300	3.0	11.9	8.6
UNL4	75 (1905)	0.25 (6)	112.5 (2858)	150 (45.72)	300	1.5	11.9	10.2
UNL5	126 (3200)	0.42 (11)	378 (9601)	150 (45.72)	300	3.0	20.0	10.6
UNL6	126 (3200)	0.42 (11)	189 (4801)	150 (45.72)	300	1.5	20.0	12.3
UNL7	180 (4572)	0.6 (15)	540 (13716)	150 (45.72)	300	3.0	28.6	12.8
UNL8	180 (4572)	0.6 (15)	270 (6858)	1800 (45720)	300	1.5	28.6	14.4

Girders S1 and S1-S were replicas of Jung and White's girders. UNL1 to UNL8 were simply supported girders proportioned so they were governed by shear failure. Length and cross-section dimensions are shown in Table 4 and span configurations in Figure 4 (b_f is flange width and t_f flange thickness).

Table 4: Girder Cross-Sectional and Length Dimensions

Test	b_f, in (mm)	t_f, in (mm)	a, ft (m)	b, ft (m)	L, ft (m)
S1	21.50 (546)	0.91 (23)	12.00 (3.66)	12.00 (3.66)	38.00 (11.58)
S1-S	21.90 (556)	0.90 (23)	12.00 (3.66)	12.00 (3.66)	38.00 (11.58)
UNL1	18.00 (457)	1.25 (32)	6.25 (1.91)	18.75 (5.72)	51.00 (15.54)
UNL2	18.00 (457)	1.25 (32)	6.25 (1.91)	9.38 (2.86)	32.25 (9.83)
UNL3	18.00 (457)	1.25 (32)	6.25 (1.91)	18.75 (5.72)	51.00 (15.54)
UNL4	18.00 (457)	1.25 (32)	6.25 (1.91)	9.38 (2.86)	32.25 (9.83)
UNL5	30.00 (762)	3.25 (83)	10.50 (3.20)	31.50 (9.60)	85.00 (25.91)
UNL6	30.00 (762)	3.25 (83)	10.50 (3.20)	15.75 (4.80)	85.00 (25.91)
UNL7	48.0 (1219)	4.5 (114)	15.75 (4.80)	47.25 (14.40)	127.00 (38.71)
UNL8	48.0 (1219)	4.5 (114)	15.75 (4.80)	23.63 (7.20)	127.00 (38.71)
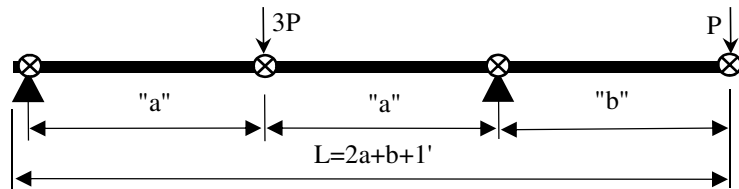
(a) Girders S1 and S1-S
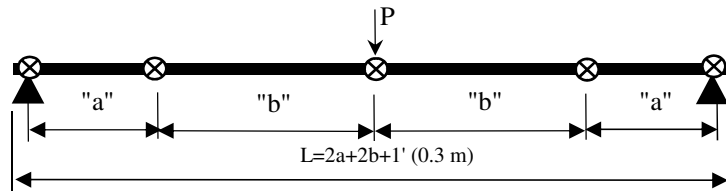
(b) Girders UNL1 to UNL8

⊗ Lateral Bracing Location ▲ support

Figure 4: Girder Layout

An eigenanalysis was performed to determine each girder's elastic shear buckling capacity followed by a fully nonlinear analysis to establish ultimate shear strength. Representative load-deflection curves are shown in Figure 5.
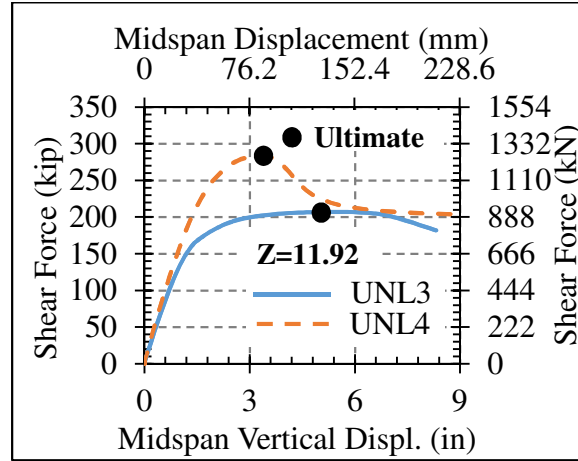
Figure 5: Applied Shear Force vs. Midspan Vertical Displacement

Shear strengths provided by the FEM analyses were then normalized against predicted capacities to evaluate horizontal curvature influence. Capacities were determined using equations founded in three separate, classical models: (1) Basler (Basler, 1961); (2) Hoglund (Hoglund, 1971, 1997); and (3) what is termed the Cardiff Model (Evans, Rockey, & Porter, 1978; Porter, Rockey, & Evans, 1975). Since each model exhibited similar trends with respect to horizontal curvature, this paper will focus on Basler's formulations. Additional information and comparisons can be found in Frankl (Frankl, 2017).

Ultimate shear capacities were determined using the shear buckling coefficient from Eq. 6 in Basler's model. For a given panel aspect ratio, the proposed shear buckling coefficient was calibrated such that nondimensionalized strength ratios exhibited accurate or conservative horizontal curvature parameters (Figure 6). These steps produced Eq. (7). For simplification purposes, Term 1, Term 2 and Term 3 correspond to the three bracketed terms in Eq. (6).

$$k_z = 0.85(\text{Term}_1) + \frac{0.85(\text{Term}_2 + \text{Term}_3)}{Z^{0.1}\left(\frac{d_o}{D}\right)} \qquad (7)$$
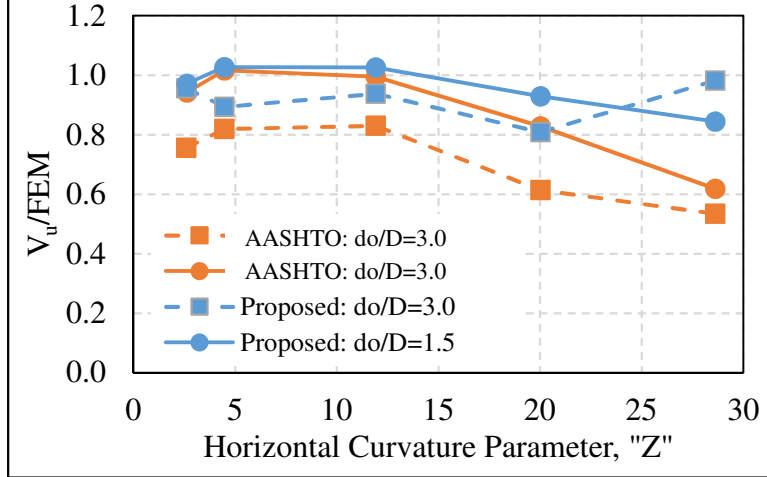
Figure 6: Normalized Shear Strengths

A version of Eq. (7) better suited to design application was developed via completion of an ANOVA over the studied range of horizontal curvature, web slenderness and panel aspect ratios. Similar to Eq. (2), Vincent's shear buckling coefficient was expanded to include an additional term addressing horizontal curvature. The resulting equation is shown in Eq. (8). More detail can be found in Frankl (Frankl, 2017).

$$k_z = 5 + \frac{5}{\left(\frac{d_o}{D}\right)^2} + \frac{3\omega}{\left(\frac{d_o}{D}\right)^2}\left(\frac{D}{t_w}\right)^{0.25} \tag{8}$$

4. Shear Buckling Coefficient Comparisons

To examine the accuracy of Eq. (2) and Eq. (8), Figure 7 compares buckling and ultimate shear strengths calculated using a modified Basler's method that incorporated the simplified and detailed shear buckling coefficients to FEM results. These figures demonstrate the degree of conservatism of the theoretical shear buckling capacity using straight girder analysis, especially at higher Z. It is also shown that the Detailed Method produces higher shear buckling capacities as Z increases in comparison to the Simplified Method. This behavior shows that Figure 7(a) shows that the simplified approach accounts for curvature reasonably well while Figure 7(b) shows that curvature could have more of an effect. Figure 7(c) and Figure 7(d) evaluate accuracy of the ultimate shear buckling capacity, modified to include curvature using the simplified and detailed shear buckling coefficients, via comparisons against fully non-linear FEM analyses of the girders in Table 4. These figures show increased conservatism when predicting shear capacity as Z increases using current AASHTO equations. Inclusion of Eq. (2) or Eq. (8) improves shear capacity predictions, with the Detailed Method providing significantly improved predictions as Z increases. The increased shear strength could help reduce girder web dimensions or increase required transverse stiffener spacing.

(a) Shear Buckling (Simplified k_s)

(b) Shear Buckling (Detailed k_s)

(c) Basler Ultimate (Simplified k_s)

(d) Basler Ultimate (Detailed k_s)
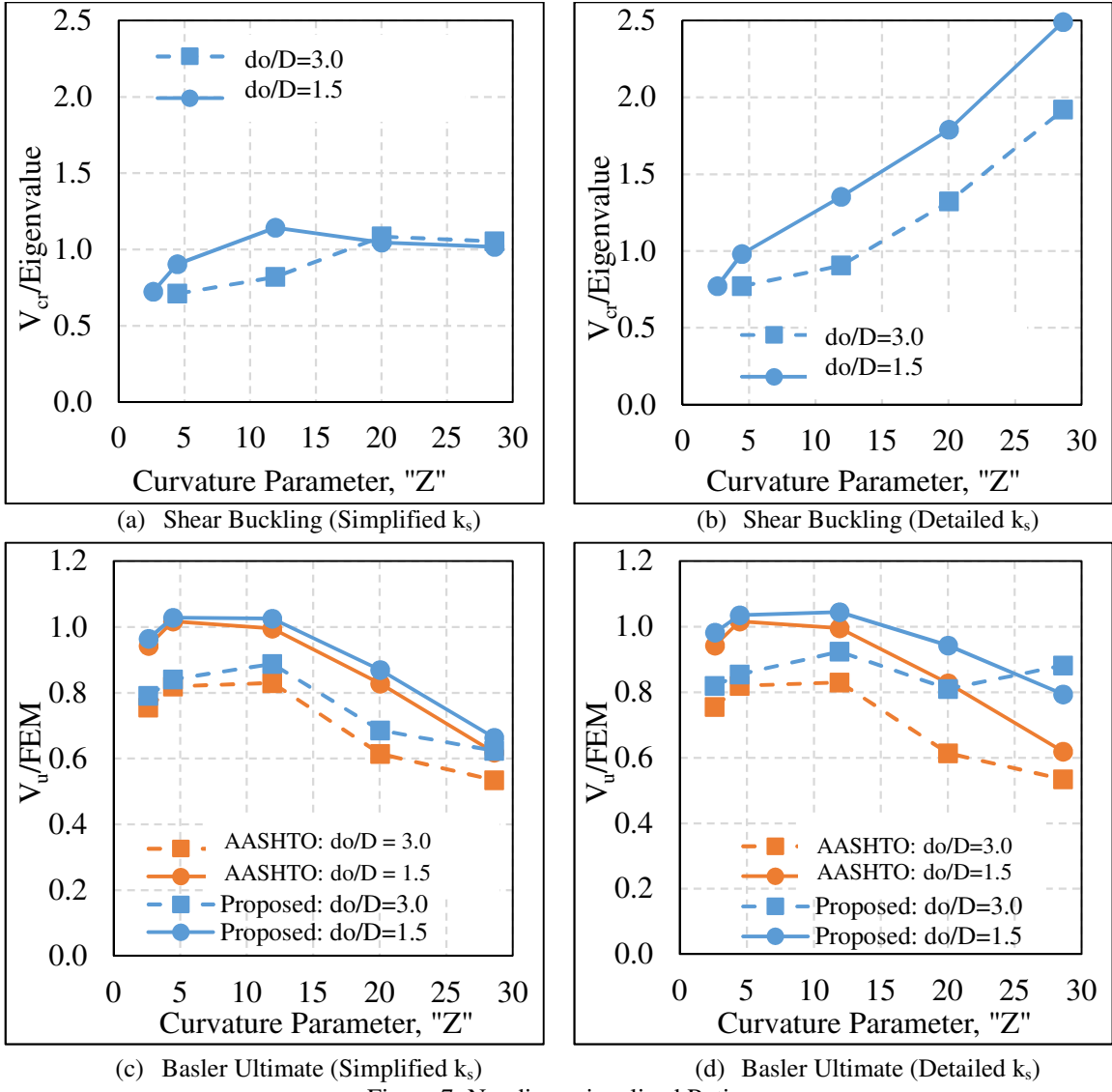
Figure 7: Nondimensionalized Ratios

Further examination of the effects of increasing transverse stiffener spacing on design optimization occurred via the completion of stiffener spacing designs for a series of girders. Designs were first completed using the current, straight girder, shear buckling coefficient and were repeated using the modified shear buckling coefficients developed herein. This process was completed for each of the ten girders in Table 4 and resulting spacings are plotted in Figure 8 for construction loads (shear buckling capacity). The figure shows that larger shear stiffener spacing could be realized as the horizontal curvature parameter increases for construction loads. A similar trend was observed for service loads (ultimate shear strength).
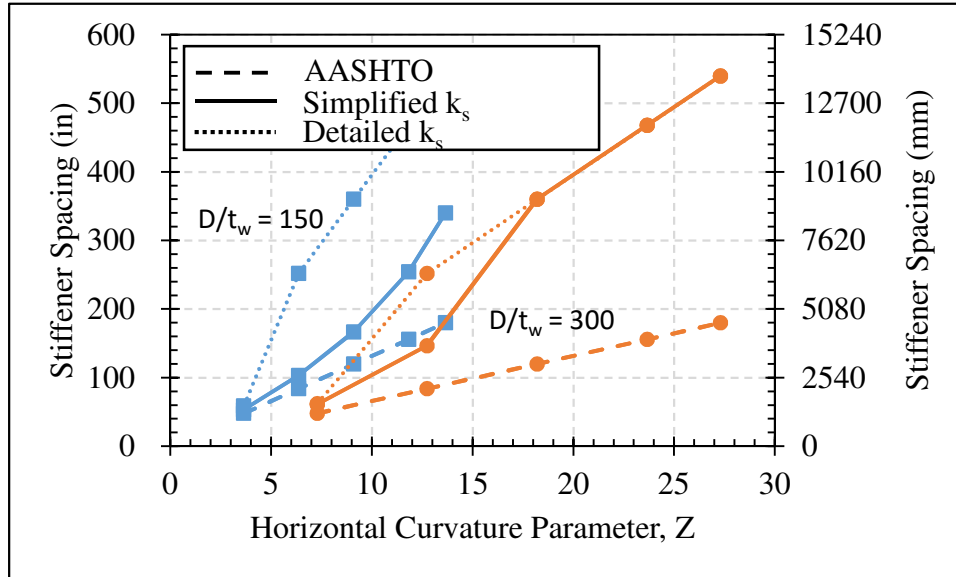
Figure 8: Shear stiffener spacing ($d_o/D = 1.0$)

5. Conclusions

This paper presents results from a larger study that examined effect of horizontal curvature on steel plate girders with slender webs. One component of the study was the development of two shear buckling coefficients that accounted for horizontal curvature. One coefficient derivation was based on a simplified approximation of Batdorf's (Batdorf et al., 1947) shear buckling coefficient curves. The other coefficient was obtained via the development of a detailed, energy-based, plate buckling solution founded in Timoshenko's seminal work that incorporated horizontal curvature into the original displacement functions.

Results from the study indicated that:

1. Batdorf's shear buckling coefficient can be approximated by adding a simplified horizontal curvature expression to AASHTO's current equation (AASHTO, 2014). This behavior showed shear strength increased with an increase in horizontal curvature (reduced radii).
2. Timoshenko's shear buckling coefficient, modified to include horizontal curvature and simplified to match current AASHTO equations, indicated that shear capacity increased with an increase in horizontal curvature (reduced radii).
3. Inclusion of horizontal curvature during shear design could increase capacity to a point where girder web plate sizes could be reduced and/or transverse stiffener spacing increased.

References

AASHTO. (2014). AASHTO LRFD bridge design specifications. *American Association of State Highway and Transportation Officials (AASHTO), Washington, DC, USA*.

ABAQUS/CAE. (2013). (Version 6.13-4).

Basler, K. (1961). *Strength of plate girders in shear* (Fritz Engineering Laboratory Report No. 251–20). Lehigh University. Retrieved from http://preserve.lehigh.edu/cgi/viewcontent.cgi?article=1069&context=engr-civil-environmental-fritz-lab-reports

Batdorf, S., Stein, M., & Schildcrout, M. (1947). *Critical shear stress of curved rectangular panels* (Technical Note No. 1348). Washington: DTIC Document.

Bleich, F. (1952). *Buckling strength of metal structures*. New York, Toronto, London: McGraw-Hill Book Company, Inc.

Culver, C. (1972). *Design recommendations for curved highway bridge report to PDOT* (Consortium of University Research Teams (CURT)). Commonwealth of Pennsylvania Department of Transporation.

de Saint-Venant, B. (1843). Mémoire sur le calcul de la résistance et de la flexion des pieces solides asimple ou adouble courbure, en prenant simultanément en consideration les divers efforts auquels elles puevent êntre soumise dans touts les sens. *CR Acad Sci Paris*, 1020–1031.

Evans, H., Rockey, K., & Porter, D. (1978). *The collapse behaviour of plate girders subjected to shear and bending*. IABSE, International Association for Bridge and Structural Engineering.

Frankl, B. (2017, August). *Buckling and Shear Capacity of Horizontally Curved Steel Plate Girders* (Dissertation). University of Nebraska-Lincoln, Lincoln, NE.

Hall, D., & Yoo, C. (1998). *Improved design specifications for horizontally curved steel girder highway bridges* (National Cooperative Highway Research Program (NCHRP)). Transportation Research Board and National Research Council.

Hibbeler, R. (2005). Mechanics of Material 6th Edition Pearson Prentice-Hall. *Upper Saddle River, NJ*.

Hoglund, T. (1971). Simply Supported Long Thin Plate I-Girders Without Web Stiffeners, Subjected to Distributed Transverse Load (Vol. 11, pp. 85–97). Presented at the IABSE Colloquium London, Reports of the Working Comissions.

Hoglund, T. (1997). Shear buckling resistance of steel and aluminium plate girders. *Thin-Walled Structures*, *29*(1), 13–30.

Issa-El-Khoury, G. (2010). *Optimization of longitudinal web stiffener location in horizontally curved plate girders* (Dissertation). The Pennsylvania State University.

Jung, S.-K., & White, D. W. (2006). Shear strength of horizontally curved steel I-girders — finite element analysis studies. *Journal of Constructional Steel Research*, *62*(4), 329–342. https://doi.org/10.1016/j.jcsr.2005.08.003

Leggett, D. (1937). The elastic stability of a long and slightly bent rectangular plate under uniform shear. *Proceedings of the Royal Society of London. Series A, Mathematical and Physical Sciences*, 62–83.

Porter, D., Rockey, K., & Evans, H. (1975). The collapse behaviour of plate girders loaded in shear. *The Structural Engineer*, *53*(8), 313–325.

Rode, H. H. (1916). *Beitrag Aur Theorie Der Knickerscheinugen* (Dissertation). Aus Christiania, Zur Zeit In Berlin.

Structural welding code - steel: aws d1.1/d1.1m. (2015). Miami: Amer Welding Society.

Vincent, G. S. (1969). *Tentative criteria for load factor design of steel highway bridges*. American Iron and Steel Institute, Committee of Structural Steel Producers [and the] Committee of Steel Plate Producers.